Microwave QR Code: An IRS-Based Solution

Sai Xu, *Member, IEEE,* Yanan Du, *Member, IEEE,* Jiliang Zhang, *Senior Member, IEEE,* and Jie Zhang, *Senior Member, IEEE*

***Abstract*—This correspondence proposes to employ intelligent reflecting surface (IRS) as an information medium to display a microwave quick response (QR) code for Internet-of-Things applications. To be specific, an IRS is used to form a dynamic bitmap image thanks to its tunable elements. With a QR code shown on the IRS, the transmitting and receiving array antennas are jointly designed to scan it by radiating electromagnetic wave as well as receiving and detecting the reflected signal. Based on such an idea, an IRS enabled information and communication system is modelled. Accordingly, some fundamental systematic operating mechanisms are investigated, involving derivation of average bit error probability for signal modulation, QR code implementation on an IRS, transmission design, detection, etc. The simulations are performed to show the achievable communication performance of system and confirm the feasibility of IRS-based microwave QR code.**

***Index Terms*—Quick response (QR) code, intelligent reflecting surface, reconfigurable intelligent surface, modulation, detection.**

I. Introduction

ALTHOUGH intelligent reflecting surface (IRS) has been widely investigated [1], almost all of the studies treat it as a pure reflection device [2], [3] or passive transmitter. To be specific, IRS is a two-dimensional metasurface, on which large numbers of electromagnetic (EM) sensitive elements are printed [4]. Compared to active antennas, the major distinction of IRS lies in that none of transmitting radio frequency (RF) chains is equipped [5]. When illuminating an IRS, the amplitude and phase of incident signal can be changed by adjusting the reflection coefficient of elements. Owing to such an appealing ability, IRS can be used as a pure reflector to construct a smart active environment to enhance or degrade signal reception [6]. Typically, IRS has been considered in multi-user communication [7], cognitive radio [8], physical layer security [8], device-to-device communication [9], multi-cell communication [10], non-orthogonal multiple access [11], ect. In addition to pure reflection, IRS is used as a passive transmitter or backscatter device [12], which is capable of sending its own information by modulating and reflecting the incoming signal. In this aspect, major investigations focus on modulation [13]–[17] and passive beamforming [18], [19]. Up to now, however, IRS has not yet been considered as an information medium, or more accurately an EM image displayer, to show a microwave quick response (QR) code for information dissemination.

As a new branch of IRS backscatter communication, IRS-based microwave QR code has some differences from the existing paradigm of passive beamforming and information transfer [13]: 1) The data bits are directly mapped to the complex reflection coefficient of the IRS elements to form a bitmap image. 2) No channel state information (CSI) is required at the IRS end. 3) Signal processing and hardware architecture at the IRS end, as well as collaboration with the transceiver, are greatly simplified. 4) The sound and systematic QR technology base facilitates practical applications of passive communication. 5) Reliable communication may still be realized with obstruction. These differences make it easy to implement microwave QR code at the IRS. Compared to conventional antenna-based communication, microwave QR code can reduce the complexities of signal processing, computing and hardware architecture at terminal devices, as well-known edge computing [20] and precoding [21] have done. Moreover, the IRS-based QR code, as an extension of QR code in microwave frequency band, has some similar advantages to the optical QR code, including but not limited to high capacity for data encoding, wide coding range, strong fault tolerance, high reliability of decoding. Therefore, microwave QR code is an ideal technology for Internet-of-Things and low-power communication scenarios, such as wireless sensor networks, smart grid, logistics management, maritime affairs, etc.

Motivated by these distinctive characteristics, this correspondence will focus on IRS-based microwave QR code, which provides a transformative means to implement wireless communication. Distinguished from [13]–[19], we attempt to present a new paradigm of backscatter communication, namely IRS-based microwave QR code, rather than investigate the IRS-related modulation technology or passive beamforming. The contributions of this correspondence are summarized as follows. 1) A concept of microwave QR code is proposed based on our recent work [19], which can be executed on an

This work was supported in part by the National Natural Science Foundation of China (62101448); in part by Project funded by the China Postdoctoral Science Foundation (2021M692649, 2022M722605); in part by the Fundamental Research Funds for the Central Universities (D5000210593); in part by the Industrial Development and Foster Project of the Yangtze River Delta Research Institute of NPU, Taicang (CY20210208).

Sai Xu (e-mail: s.xu@sheffield.ac.uk, xusai@nwpu.edu.cn) is with the Department of Electronic and Electrical Engineering, University of Sheffield, Sheffield, S10 2TN, UK, and was with the School of Cybersecurity, Northwestern Polytechnical University, Xi'an, Shaanxi, 710072, China during this work. Yanan Du (e-mail: duyanan@nwpu.edu.cn) is with the School of Cybersecurity, Northwestern Polytechnical University, Xi'an, Shaanxi, 710072, China. Jiliang Zhang (e-mail: jiliang.zhang@sheffield.ac.uk) is with College of Information Science and Engineering, Northeastern University, Shenyang, Liaoning, 314001, China, and was with Department of Electronic and Electrical Engineering, University of Sheffield, Sheffield, S10 2TN, UK and Ranplan Wireless Network Design Ltd., Cambridge, CB23 3UY, UK during this work. Jie Zhang (e-mail: jie.zhang@sheffield.ac.uk) is with the Department of Electronic and Electrical Engineering, University of Sheffield, Sheffield, S10 2TN, UK, and also with Ranplan Wireless Network Design Ltd., Cambridge, CB23 3UY, UK. (*corresponding author: Jiliang Zhang*)

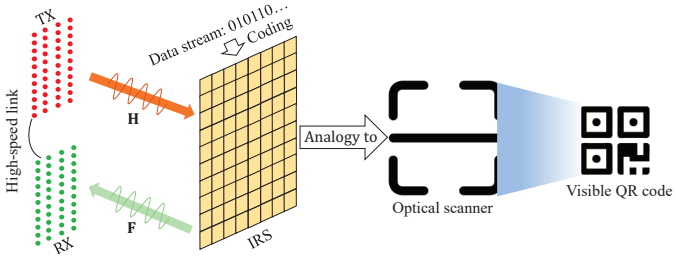

Fig. 1. An illustration of the proposed IRS enabled information and communication system, where an IRS acts as an element image displayer to map the information to the complex reflection coefficient of its elements.

IRS, but not limited to it. The proposed system framework also applies to other cases of coded image, in addition to QR code. 2) Fundamental systematic operating mechanisms are preliminarily presented, including signal modulation, QR code implementation, transmission design, detection, etc. 3) Simulations are performed to show the feasibility of the proposed system and schemes, which are able to provide useful guidelines to inspire future research.

II. System Model

Consider an IRS enabled information and communication system as shown in Fig. 1, where an IRS builds up an element image carrying data information instead of a pure reflector for radio signal, while the transmitting array antennas (TXs) radiate EM wave towards the IRS and the receiving array antennas (RXs) detect the echo signal for data extraction. The TXs and the RXs may be deployed centrally or separately. In either case, the TXs and the RXs can exchange information smoothly through a high-speed link, which ensures that they can collaborate to read the information on the IRS. Moreover, the interference between the TXs and the RXs can be well eliminated[1]. The relationship between the TXs/RXs and the IRS is in analogy with that between an optical scanner and a visible QR code.

Let N_{t}, N_{r} and L denote the numbers of the TXs, the RXs and the elements of the IRS, respectively. It is assumed that all CSIs are perfectly known with quasi-static fading. $\mathbf{H} \in \mathbb{C}^{L\times N_{\mathrm{t}}}$ and $\mathbf{F} \in \mathbb{C}^{N_{\mathrm{r}}\times L}$ denote the channel gain matrices from the TXs to the IRS and from the IRS to the RXs, respectively. When the TXs radiate EM wave bearing no information[2], each IRS can passively modulate its information to the reflected signal with time-varying reflection coefficient of each element. Mathematically, the modulation process at the IRS is modelled as

$$\mathbf{F}\boldsymbol{\Theta}\mathbf{H}\mathbf{w} = \mathbf{F}\mathrm{diag}\{\mathbf{H}\mathbf{w}\}\boldsymbol{\theta}, \tag{1}$$

where $\mathbf{w}$ is the beamforming vector at the TXs. $\boldsymbol{\Theta}$ and $\boldsymbol{\theta}$ are respectively the diagonal matrix of reflection coefficient and the corresponding vector, with $\boldsymbol{\Theta} = \mathrm{diag}\{\boldsymbol{\theta}\}$. $\boldsymbol{\theta}$ is an information vector rather than a passive beamforming vector, where each of its vector elements is not more than one.

[1]The interference elimination can be realized by physical separation between the TXs and the RXs or advanced signal processing techniques [22].

[2]All the transmitted data symbols from the TXs are set as one since no information is sent.

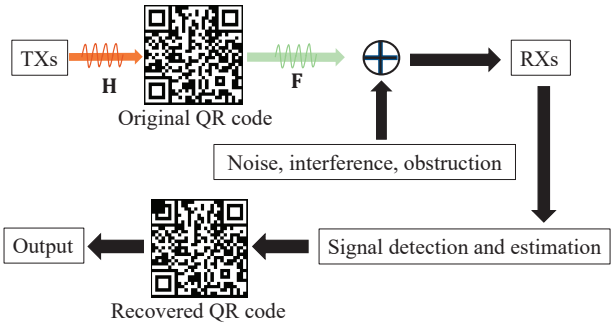

Fig. 2. An illustration of the principle of IRS enabled QR code communication.

Therefore, $\left[\boldsymbol{\theta}\boldsymbol{\theta}^H\right]_{l,l} \leq 1$ holds, where $[\cdot]_{l,l}$ denotes the l-th diagonal element of matrix. Based on this model, the received signal at the RXs is given by

$$\mathbf{y} = \mathbf{F}\mathrm{diag}\{\mathbf{H}\mathbf{w}\}\boldsymbol{\theta} + \mathbf{z}, \tag{2}$$

where $\mathbf{z}$ is white Gaussian noise vector with $\mathbf{z} \sim (\mathbf{0}, \sigma^2\mathbf{I})$.

The performance of the considered IRS enabled information and communication system is highly dependent on the amplitude and phase of each element. Moreover, the number of antennas at the RXs has a huge impact on the detection of the echo signal and the information acquisition. In the following sections, we will investigate two related agendas for the considered system, including average bit error probability (ABEP) of signal modulation and IRS enabled QR code communication.

III. Derivation of ABEP

This section will compute the average symbol error probability (ASEP) for the considered IRS enabled information and communication system according to the information theory. Based on the ASEP, the ABEP of phase shift keying (PSK) as a typical modulation example is obtained, considering that the amplitude adjustment of elements at the IRS has a high control complexity[3].

Specifically, let $\mathbf{V} = \mathbf{F}\mathrm{diag}\{\mathbf{H}\mathbf{w}\}$ and $\mathbf{U} = [\mathbf{V}^H\mathbf{V}]^{-1}\mathbf{V}^H$. Based on (2), the output of the received signal at the RXs is given by

$$\mathbf{y}' = \boldsymbol{\theta} + \mathbf{z}', \tag{3}$$

where $\mathbf{y}' = \mathbf{U}\mathbf{y}$ and $\mathbf{z}' = \mathbf{U}\mathbf{z}$. For the l-th element of the IRS, the corresponding output of the received signal is given by

$$\mathbf{y}'(l) = \boldsymbol{\theta}(l) + \mathbf{z}'(l). \tag{4}$$

It is assumed that the phase of each element at the IRS constructs a signal constellation diagram of size M, denoted by $\mathcal{X} = \{x_1, x_2, \cdots, x_M\}$, with all constellation points having the same occurrence probability. Therefore, the maximum likelihood (ML) estimate of $\boldsymbol{\theta}(l)$ is given by

$$\hat{\boldsymbol{\theta}}(l) = \arg\min_{x_m\in\mathcal{X}} |\mathbf{y}'(l) - x_m|. \tag{5}$$

Then, the closed-form expression of ASEP for the l-th element

[3]Modulation is not the research focus of this work. For more advanced IRS modulation schemes, please kindly refer to [13], [14].

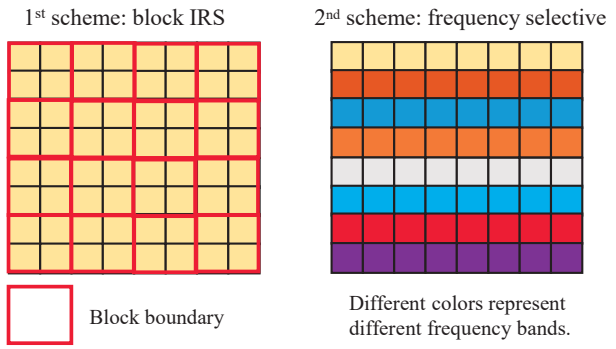

Fig. 3. Two schemes to cope with the insufficient antennas at the RXs.

of the IRS is given by

$$\mathrm{P}_{\mathrm{ASEP}}(l)=\sum_{m=1}^{M}\sum_{\hat{m}=1,\hat{m}\neq m}^{M}\frac{\Pr\left\{\hat{\boldsymbol{\theta}}(l)=x_{\hat{m}}|\boldsymbol{\theta}(l)=x_m\right\}}{M}. \quad (6)$$

Based on (6), the closed-form expression of ABEP for the l-th element of the IRS can be obtained. When each element of the IRS switches only between two states, the low-complexity modulation of BPSK is an excellent choice. For BPSK, the ABEP for the l-th element of the IRS is given by[4]

$$\mathrm{P}_{\mathrm{ABEP,\ BPSK}}(l)=Q\left(\sqrt{\frac{2}{\mathbf{C}_{ll}}}\right), \quad (7)$$

where $\mathbf{C}_{ll}$ is the (l,l)-th element of $\mathbf{C}=\sigma^2\mathbf{U}\mathbf{U}^H$. When more phase states can be adjusted for each element, more information is contained at a fixed-size IRS. For QPSK, the ABEP for the l-th element of the IRS is approximately given by

$$\mathrm{P}_{\mathrm{ABEP,\ QPSK}}(l)\approx Q\left(\sqrt{\frac{1}{\mathbf{C}_{ll}}}\right). \quad (8)$$

When the number of phase states is greater than four, the ABEP for the l-th element of the IRS is approximately given by

$$\mathrm{P}_{\mathrm{ABEP,\ }M\text{-PSK}}(l)\approx\frac{2}{\log_2 M}\left[Q\left(\sqrt{\frac{1-\cos(2\pi/M)}{\mathbf{C}_{ll}}}\right)+Q\left(\sqrt{\frac{1-\cos(4\pi/M)}{\mathbf{C}_{ll}}}\right)\right],\ M>4. \quad (9)$$

IV. IRS Enabled QR Code Communication

This section will discuss how an IRS acting as a microwave QR code displayer interacts with the TXs/RXs, involving QR code implementation, transmission design, detection, etc. The operating principle is depicted in Fig. 2. Considering that there are many versions for QR code to support different languages, numbers, letters or their mixture and that QR coding is an independent field of study, the QR coding design is beyond the scope of this correspondence.

At the TXs, channel estimation and beamforming design have a huge effect on the communication performance of system. Since IRS acts as an information medium with each element having the identical constellation diagram, $\boldsymbol{\Theta}=\mathbf{I}$ is set as the precondition for channel estimation and beamforming. Under such a precondition, it is easy to estimate the cascaded channel $\mathbf{F}\boldsymbol{\Theta}\mathbf{H}$, that is $\mathbf{F}\mathbf{H}$. Based on the CSI of $\mathbf{F}\mathbf{H}$, a straightforward beamforming scheme is adopted, where $\mathbf{w}$ is designed as the eigenvector corresponding to the largest eigenvalue of the matrix $\mathbf{H}^H\mathbf{F}^H\mathbf{F}\mathbf{H}$.

At the RXs, the number of antennas may be far smaller than that of the IRS elements in practice, which results in the difficulty in the signal detection. To address this issue, two schemes may be considered, as illustrated in Fig. 3. In the first scheme, an IRS is equally divided into N_{r} blocks while all elements in a block have the same reflection coefficient [18]. As a result, the independent IRS elements are reduced into N_{r}, and each IRS block can reflect more power towards the RXs than one element. If the number of the IRS blocks is insufficient to bear a complete message, QR codes carried by multiple frames on the IRS are merged into one for information transfer. In the second scheme, frequency division multiplexing is employed. To be specific, an IRS is made up of multiple groups of frequency selective elements for interference elimination and each group is able to reflect the EM wave in a specific frequency band. Based on this scheme, the signal reflected by different groups of elements can be detected by the RXs at the same time.

Relying on different modulation schemes, each element or IRS block is used as one or multiple QR modules. For example, when BPSK is adopted, one element or IRS block represents one QR module; when 16-PSK is adopted, one element or IRS block represents four QR modules. When the EM wave from the TXs impinges on the IRS, the information carried by each element is modulated into the reflected signal. Then, the signal is received, detected and estimated at the RXs. Due to noise, interference and obstruction, the recovered QR code may be impaired. Even so, the information can still be correctly decoded under a certain impaired level.

V. Numerical Results

This section will evaluate the feasibility and the achievable performance of the proposed IRS enabled information and communication system by numerical simulations. In simulations, the channels $\mathbf{H}$ and $\mathbf{F}$ are randomly generated from the Rician channel distribution with the Rician factor κ, where the path loss at the transmission distance d is given by $\mathrm{PL}=\mathrm{PL}_0-25\lg(d/d_0)$ dB with PL_0 = -30 dB at the reference distance d_0 = 1m. The legend `PSK` represents the schemes of PSK with multiple modulation orders considered, while `Theo` and `Simu` denote the theoretical and simulation results, respectively. Some constant parameters are set as: the distance from the TXs/RXs to the IRS d_{I} = 50 m, the noise temperature T = 300 K, and the noise bandwidth B = 1 MHz.

Fig. 4 depicts how the ABEPs of multiple modulation schemes of PSK depend on the average signal-to-noise ratio (SNR), the number of antennas at the TXs and the Rician factor of channels, where N_{t} = 64, N_{r} = 64, L = 64, κ = 0.1,

[4]The equations (7), (8) and (9) can be easily obtained according to Sections 6.1.2 and 6.1.3 of [23].

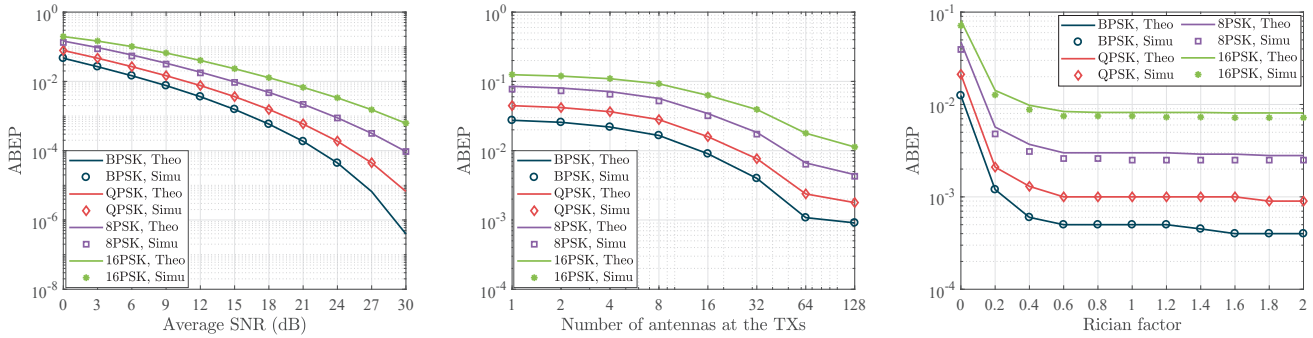

Fig. 4. The impact of the average SNR, the number of antennas at the TXs and the Rician factor of channels on the ABEPs of multiple modulation schemes of PSK.

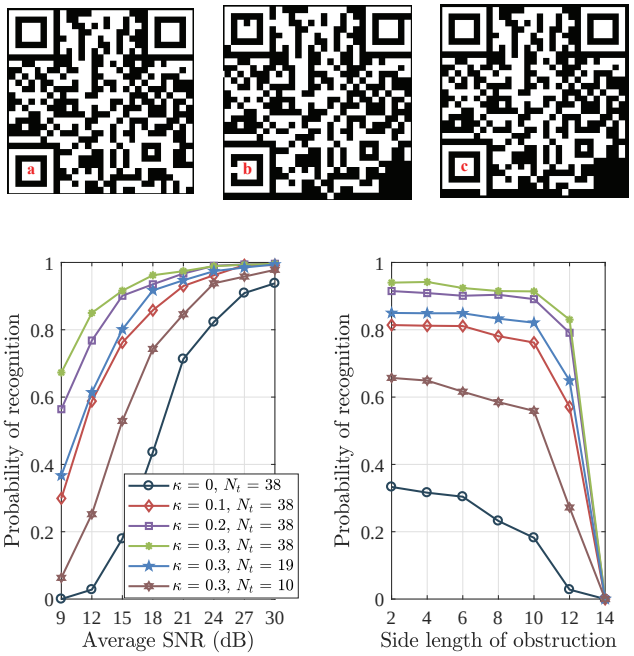

Fig. 5. The impact of the average SNR, the side length (measured by number of elements) of obstruction, the number of antennas at the TXs and the Rician factor on the recognition probability of QR code for BPSK, where (a), (b) and (c) are the original QR code, the recovered unrecognizable QR code and the recovered recognizable QR code, respectively.

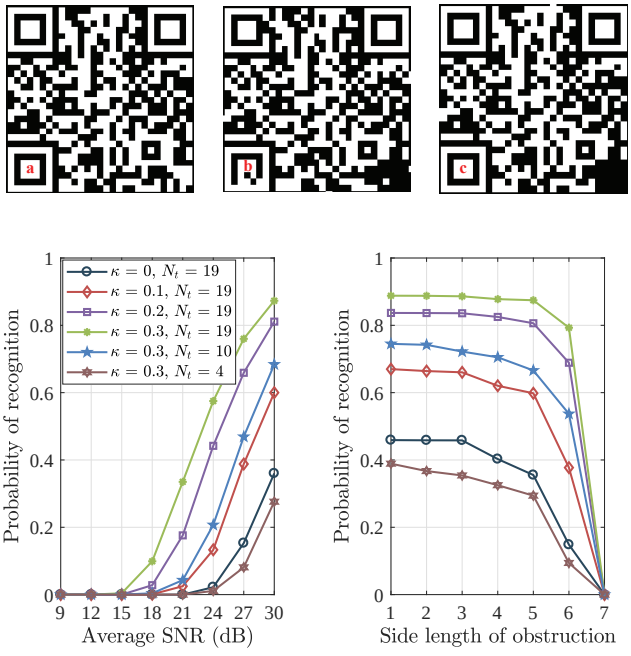

Fig. 6. The impact of the average SNR, the side length (measured by number of elements) of obstruction, the number of antennas at the TXs and the Rician factor on the recognition probability of QR code for 16-PSK, where (a), (b) and (c) are the original QR code, the recovered unrecognizable QR code and the recovered recognizable QR code, respectively.

the average SNR γ = 15 dB, if N_{t}, κ and γ are not used as X-axis variables. It is clearly seen that all curves decline with the average SNR, the number of antennas at the TXs and the Rician factor increasing. Moreover, the curves of `Theo` almost coincide with `Simu` in all modulation schemes of PSK, which indicates that the theoretical approximation is quite accurate. By comparison, the BPSK achieves the lowest ABEP and an increase in modulation order of PSK lifts the ABEP.

Figs. 5 and 6 show how the average SNR, the side length (measured by number of elements) of obstruction, the number of antennas at the TXs and the Rician factor affect the recovery and recognition probabilities of QR code for BPSK and 16-PSK, where N_{t} = 38, N_{r} = 38, $L = 38^2$, γ = 15 dB, the side length of obstruction D = 10 for BPSK and N_{t} = 19, N_{r} = 19, $L = 19^2$, γ = 30 dB, D = 5 for 16-PSK are set. The obstruction is assumed to be square and the right bottom corner of the IRS is blocked. All QR codes shown are from a random observation for BPSK and 16-PSK. It is seen that an increase in the average SNR, the number of antennas at the TXs and the Rician factor contributes to improving the recognition probability of QR code, while the side length of obstruction does the reverse.

VI. Conclusions

This correspondence proposed to employ IRS-based microwave QR code for passive radio communication and investigated some fundamental agendas, involving the ABEP for signal modulation, QR code implementation on an IRS, transmission design, detection, etc. According to the theoretical analysis and simulation results, it can be concluded that: 1) IRS-based microwave QR code achieves a satisfactory communication performance, thereby being feasible; 2) BPSK has the lowest ABEP, and an increase in modulation order of PSK lifts the ABEP with the elements for displaying QR

code reduced; 3) A higher average SNR, more antennas at the TXs and a larger Rician factor contribute to lowering the ABEP and increasing the probability of recognizing QR code; 4) IRS-based microwave QR code has a good robustness to obstruction.

REFERENCES

[1] S. Gong, *et al.*, "Toward smart wireless communications via intelligent reflecting surfaces: A contemporary survey," *IEEE Commun. Surveys Tuts.*, vol. 22, no. 4, pp. 2283-2314, 4th Quart., 2020

[2] H. Zhang, B. Di, L. Song, and Z. Han, "Reconfigurable intelligent surfaces assisted communications with limited phase shifts: How many phase shifts are enough?," *IEEE Trans. Veh. Technol.*, vol. 69, no. 4, pp. 4498-4502, Apr. 2020.

[3] B. Di, H. Zhang, L. Song, Y. Li, Z. Han, and H. V. Poor, "Hybrid beamforming for reconfigurable intelligent surface based multi-user communications: Achievable rates with limited discrete phase shifts," *IEEE J. Sel. Areas Commun.*, vol. 38, no. 8, pp. 1809-1822, Aug. 2020.

[4] Q. Wu, and R. Zhang, "Towards smart and reconfigurable environment: Intelligent reflecting surface aided wireless network," *IEEE Commun. Mag.*, vol. 58, no. 1, pp. 106-112, Jan. 2020.

[5] S. Xu, J. Liu, T. K. Rodrigues, and N. Kato "Envisioning intelligent reflecting surface empowered space-air-ground integrated network," *IEEE Netw.*, vol. 35, no. 6, pp. 225-232, Nov./Dec. 2021.

[6] M. D. Renzo, *et al.*, "Smart radio environments empowered by reconfigurable intelligent surfaces: How it works, state of research, and the road ahead," *IEEE J. Sel. Areas Commun.*, vol. 38, no. 11, pp. 2450-2525, Nov. 2020.

[7] S. Zhang, and R. Zhang, "Intelligent reflecting surface aided multi-user communication: Capacity region and deployment strategy," *IEEE Trans. Commun.*, vol. 69, no. 9, pp. 5790-5806, Sep. 2021.

[8] S. Xu, J. Liu, Y. Cao, J. Li, and Y. Zhang, "Intelligent reflecting surface enabled secure cooperative transmission for satellite-terrestrial integrated networks," *IEEE Trans. Veh. Technol.*, vol. 70, no. 2, pp. 2007-2011, Feb. 2021.

[9] S. Mao, X. Chu, Q. Wu, L. Liu, and J. Feng, "Intelligent reflecting surface enhanced D2D cooperative computing,"*IEEE Wireless Commun. Lett.*, vol. 10, no. 7, pp. 1419-1423, Jul. 2021.

[10] A. A. Khan, and R. S. Adve, "Centralized and distributed deep reinforcement learning methods for downlink sum-rate optimization," *IEEE Trans. Wireless Commun.*, vol. 19, no. 12, pp. 8410-8426, Dec. 2020.

[11] Z. Ding, and H. Vincent Poor, "A simple design of IRS-NOMA transmission," *IEEE Commun. Lett.*, vol. 24, no. 5, pp. 1119-1123, May 2020.

[12] W. Tang, *et al.*, "MIMO transmission through reconfigurable intelligent surface: system design, analysis, and implementation," *IEEE J. Sel. Areas Commun.*, vol. 38, no. 11, pp. 2683-2699, Nov. 2020.

[13] S. Guo, S. Lv, H. Zhang, J. Ye, and P. Zhang, "Reflecting modulation," *IEEE J. Sele. Areas Commun.*, vol. 38, no. 11, pp. 2548-2561, Nov. 2020.

[14] L. Yang, F. Meng, M. O. Hasna, and E. Basar, "A novel RIS-assisted modulation scheme," *IEEE Wireless Commun. Lett.*, vol. 10, no. 6, pp. 1359-1363, Jun. 2021.

[15] E. Basar, "Reconfigurable intelligent surface-based index modulation: A new beyond MIMO paradigm for 6G," *IEEE Trans. Commun.*, vol. 68, no. 5, pp. 3187-3196, May 2020.

[16] Q. Li, M. Wen, and M. Di Renzo, "Single-RF MIMO: From spatial modulation to metasurface-based modulation," *IEEE Wireless Commun.*, vol. 28, no. 4, pp. 88-95, Aug. 2021.

[17] W. Tang, *et al.*, "Wireless communications with programmable metasurface: New paradigms, opportunities, and challenges on transceiver design," *IEEE Wireless Commun.*, vol. 27, no. 2, pp. 180-187, Apr. 2020.

[18] S. Xu, Y. Du, J. Liu, and J. Li, "Intelligent reflecting surface based backscatter communication for data offloading," *IEEE Trans. Commun.*, vol. 70, no. 6, pp. 4211-4221, Jun. 2022.

[19] S. Xu, Y. Du, J. Zhang, J. Wang, and J. Zhang, "An IRS backscatter enabled integrated sensing, communication and computation system," 2022, *arXiv*: 2207.10219. [Online]. Available: https://doi.org/10.48550/arXiv.2207.10219

[20] P. Mach, and Z. Becvar, "Mobile edge computing: A survey on architecture and computation offloading," *IEEE Commun. Surveys Tuts.*, vol. 19, no. 3, pp. 1628-1656, 3rd Quart. 2017.

[21] M. Agiwal, A. Roy, and N. Saxena, "Next generation 5G wireless networks: A comprehensive survey," *IEEE Commun. Surveys Tuts.*, vol. 18, no. 3, pp. 1617-1655, 3rd Quart. 2016.

[22] A. Sabharwal, P. Schniter, D. Guo, D. W. Bliss, S. Rangarajan, and R. Wichman, "In-band full-duplex wireless: Challenges and opportunities," *IEEE J. Sel. Areas Commun.*, vol. 32, no. 9, pp. 1637-1652, Sep. 2014.

[23] A. Goldsmith, *Wireless Communications*. New York, NY, USA: Cambridge University Press, 2005.